Recent star formation in nearby galaxies from GALEX imaging: M101 and M51

Luciana Bianchi[1], David A. Thilker[1], Denis Burgarella[4], Peter G. Friedman[2], Charles G. Hoopes[1], Samuel Boissier[7], Armando Gil de Paz[7], Tom A. Barlow[2], Yong-Ik Byun[3], Jose Donas[4], Karl Forster[2], Timothy M. Heckman[1], Patrick N. Jelinsky[6], Young-Wook Lee[3], Barry F. Madore[7], Roger F. Malina[4], D. Christopher Martin[2], Bruno Milliard[4], Patrick Morrissey[2], Susan G. Neff[9], R. Michael Rich[10], David Schiminovich[2], Oswald H. W. Siegmund[6], Todd Small[2], Alex S. Szalay[1], Barry Y. Welsh[6], Ted K. Wyder[2]

ABSTRACT

The GALEX (Galaxy Evolution Explorer) Nearby Galaxies Survey is providing deep far-UV and near-UV imaging for a representative sample of galaxies in the local universe. We present early results for M51 and M101, from GALEX UV imaging and SDSS optical data in five bands. The multi-band photometry of compact stellar complexes in M101 is compared to population synthesis models, to derive ages, reddening, reddening-corrected luminosities and current/initial masses. The GALEX UV photometry provides a complete census of young compact complexes on a $\approx$ 160 pc scale. A galactocentric gradient of the far-UV - near-UV color indicates younger stellar populations towards the outer parts of the galaxy disks, the effect being more pronounced in M101 than in M51.

[1]Deptartment of Phys.& Astron., Johns Hopkins University,3400 N.Charles St., Baltimore, MD21218 (bianchi,dthilker,hoopes,heckman@pha.jhu.edu)

[2]California Inst. of Technology,MC405-47,1200 E.California Blvd, Pasadena, CA91125 (friedman,tab,krl,cmartin,patrick,ds,tas,wyder@srl.caltech.edu)

[3]Center for Space Astrophysics, Yonsei University, Seoul 120-749, Korea (byun,ywlee@obs.yonsei.ac.kr)

[4]Laboratoire d'Astrophysique de Marseille, BP8, Traverse du Siphon, 13376 Marseille Cedex 12,FR (denis.burgarella,roger.malina,bruno.milliard@oamp.fr)

[6]Space Sciences Laboratory, University of California at Berkeley, 601 Campbell Hall, Berkeley, CA 94720 (patj,ossy,bwelsh@ssl.berkeley.edu)

[7]Observatories of the Carnegie Institution of Washington, 813 Santa Barbara St., Pasadena, CA 91101 (agpaz,barry@ipac.caltech.edu)

[9]Laboratory for Astronomy and Solar Physics, NASA Goddard Space Flight Center, Greenbelt, MD 20771 (neff@stars.gsfc.nasa.gov)

[10]Department of Physics and Astronomy, University of California, Los Angeles, CA 90095 (rmr@astro.ucla.edu)

Subject headings: galaxies: —individual (M51, M101) —galaxies: star clusters —galaxies: star formation —ultraviolet: galaxies

1. Introduction

The study of stellar cluster systems and compact associations provides insight into a galaxy's star-formation history and stellar content. Far-UV and near-UV bands are a sensitive probe for detection of young stellar clusters, and for measurement of their physical parameters and - combined with optical data - of their extinction (Bianchi et al. 1999, Chandar et al. 1999).

The GALEX Nearby Galaxies Survey (NGS), described by Bianchi et al. (2004a, b) is providing deep far-UV (FUV) and near-UV (NUV) imaging for a representative sample of ≈ 200 galaxies in the local universe. We present early GALEX NGS data of M101 and M51. We also use five-band optical imaging from the Sloan Digital Sky Survey (SDSS). We derive ages, reddening, and current/initial masses for the compact UV sources in M101 (Sect. 3). Radial profiles of UV brightness and color are presented in Sect. 4.

The two galaxies studied in this paper have been previously imaged in a broad far-UV band ($\lambda_{eff} \approx 1521$Å) by the *Ultraviolet Imaging Telescope* (UIT). The UIT data were analysed by Kuchinski et al. (2000), Waller et al. 1997 (M101), Hill et al. 1997 (M51), Hoopes, Walterbos, & Bothun (2001). While the UIT FUV images revealed morphological differences with respect to the optical bands, and the brightest stellar complexes, the GALEX data yield significant advances. First, both FUV and NUV bands are available, providing an essentially reddening-free color which gives a direct indication of the age (for compact sources) independent of the extinction estimate, while the UV-to-optical wide baseline is very sensitive to both extinction and age (Sect. 3). Second, GALEX's detectors afford greater sensitivity and linearity than the UIT data (which were recorded on film), measuring UV emission out to larger disk radii, and down to fainter (by about 3 mag) fluxes (Sect. 4).

2. Observations and Data Analysis

The GALEX instrument is described by Martin et al. (2004, this issue) and its on-orbit performance by Morrissey et al. (2004, this issue). GALEX FUV (1350–1750 Å) and NUV (1750–2750 Å) imaging was obtained with total exposure times of 1414 and 1041 sec for M51 and M101. Assuming distances of 9.6 Mpc, and 7.4 Mpc (M51: Sandage & Tammann 1974, M101: Kelson et al. 1996) the 4.6″ FWHM GALEX PSF corresponds to 209, and 157 pc.

The 1-σ (at the PSF scale) NUV(FUV) sensitivity limit of the GALEX images is 27.9 (27.8) AB mag $''^{-2}$ for M51 and 27.6 (27.5) AB mag $''^{-2}$ for M101.

We also used SDSS imaging of M51 and M101 in the *ugriz* filters. The resolution of the optical data (1-2″, $\approx$ 70 and 50 pc for M51 and M101 respectively) is superior to that of GALEX, and in some cases the GALEX UV sources are resolved into two or three optical sources. The different angular resolutions were taken into account when matching the UV and optical sources. For the analysis in Sect. 3, we focus on the smallest scale detections in each galaxy, thus sampling the star forming complexes in M101 and M51 on a scale corresponding to the GALEX resolution. Post-pipeline processing and photometry on the GALEX and SDSS images were performed using the SEXTRACTOR (Bertin & Arnouts 1996) and IRAF APPHOT packages. To obtain our master list of "point-like" sources we first ran SEXTRACTOR on the NUV imagery after removal of the diffuse background, using a detection kernel matched to the GALEX NUV PSF (4.6″). The background was estimated using a circular median-filter of diameter 10.5″ (7 pixels). Such background removal is crucial in order to obtain a complete SEXTRACTOR catalog in bright regions of M51 and M101. We then passed this list of compact NUV sources to the APPHOT package, running PHOT (with recentering enabled) on background subtracted versions of the GALEX FUV, NUV, and convolved SDSS images. Sources which shifted in position by more than 4″ in any band were eliminated. Finally, PHOT was used to measure fluxes for all surviving compact sources with 4″ aperture radius, and aperture corrections based on isolated field stars were applied. Figures 1 and 2 show the GALEX NUV image for the two galaxies. The matched sources with photometric errors better than 0.2 mag in the UV bands are shown. Table 1 gives the number of detected sources in each band and the statistics of sources for given error limits.

The final matched catalog was based on the NUV source list (the deepest UV band), and includes only NUV sources having a counterpart in at least one other band. The photometry procedures were verified by comparing our results with both GALEX and SDSS pipeline photometry on portions of the same images outside the galaxy body, where the standard pipeline results are reliable. We found complete consistency within the errors. We applied our photometry technique in the regions containing the galaxies, where the standard GALEX and SDSS pipelines break down. We use the flux calibration from the GALEX Internal Release version 0.2.

3. The physical parameters of the compact complexes

The measured colors for the compact UV sources in M101 were compared to synthetic colors computed from the Bruzual and Charlot (2003) models for Integrated Populations, for

the cases of Single Burst (hereafter SSP) and of Continuous Star Formation (hereafter CSP), as a function of age. As expected (because we are sampling UV-bright compact complexes) most sources are better represented by a SSP SED. In this work we assume solar metallicity and a Chabrier (2003) IMF (mass range 0.1 - 100 $\mathcal{M}_{\odot}$). Because the UV sources are mostly very young complexes, the analysis is not very sensitive to metallicity. For instance, the *FUV* -*NUV* color of a SSP model with solar metallicity for 1, 10, and 100 Myrs is *FUV* -*NUV* = -0.35, -0.06, 0.18 (in the AB mag system). The model colors for the same ages at z=0.008 differ by $\leq$0.1, which leads to an uncertainty in the age by up to a factor of 3, and typically by $\leq$2, depending on the age. According to the HII regions study by Kennicutt, Bresolin, & Garnett (2003), solar metallicity is appropriate out to $\approx 6'$, which includes the majority of our sources.

Figure 3 shows color-color diagrams of the sources compared to the models. We derived physical parameters by comparing the measured magnitudes to the model colors. Because the observed SED's depend on the cluster age (intrinsic SED) and on the wavelength-dependent interstellar extinction, we reddened the model colors for different amounts of extinction and reddening types. Two different methods were used, and the results compared. In the first method, we used the GALEX measurements alone, and estimated the cluster ages by comparing the *FUV* -*NUV* color to the models. Reddening has a negligible effect on the *FUV* -*NUV* color, for E(B-V) values associated with these galaxies. For instance, model colors for E(B-V)=0.2 (MW-type extinction, R_V=3.1) differ from the unreddened colors by ≤ 0.01, up to 100Myrs. In the second method, we fit all the measured multi-band magnitudes with the synthetic colors to derive age and E(B-V) concurrently, by χ^2 minimization, taking into account the photometric errors in each band (see Bianchi et al. 2004 in prep., for more details).

Ages determined from the *FUV* -*NUV* color, and by the SED fit of the UV-to-optical bands respectively, agree for most of the sources within the errors, but are discrepant for some sources, where a color gradient may be present. We adopt the age from the SED fits, which represents the average over the area included in the aperture, for the sources with errors <0.05-0.10 mag (SDSS and GALEX bands respectively). These ages are shown in the green-dashed histogram in Figure 4, and ages derived by the *FUV* -*NUV* color only (for the UV sources with *FUV* and *NUV* errors <0.2 mag) are shown by the blue (solid) histogram. This sample (about 1100 sources) includes a large number of (mostly younger) sources eliminated by the error cuts in the SED-fit sample. We note that individual errors in the ages derived by the *FUV* -*NUV* color in the range of log age (in yrs) =6.5-7.5 may be larger than the bin-size, as *FUV* -*NUV* does not vary appreciably in this range. For this reason, and for the selection effects limiting the sources with good SED fits, we do not attempt to interpret this histogram in terms of star-formation history. We point out however the great sensitivity of the GALEX

UV imaging to detect and measure the youngest sources. The sharp decline in the number of sources at older ages is mostly due to our magnitude limits and color selection effect. However, disruption may be more effective for these large-scale complexes than for bound clusters. Once reddening and age are determined for each complex, the reddening-corrected luminosity and age yield the current (and thus the initial) mass, by comparison with the same models (Figure 4, lower panel). Figure 4 also shows the cluster sample detected in one HST WFPC2 field with U, B, V, I measurements by Chandar et al. (2004, in preparation) in M101. Given the higher spatial resolution, the HST photometry samples bound stellar clusters, while our GALEX census samples the star forming complexes on spatial scales of $\lesssim$ 160 pc. For M51 we do not perform a similar analysis given the smaller number of compact sources detected, and distortion of the images which limits the accuracy of compact sources photometry.

In summary, the GALEX images provided a complete census of young, compact star-forming complexes. The UV bands are extremely sensitive to young stellar populations. E.g., the [intrinsic] FUV-r ($\approx$ FUV-V) colors of clusters (SSP) with ages of 1, 10, 100 Myrs are -1.78, -0.30, 1.11 (AB mag), while the $u-g$ ($g-r$) [approximately B-V (U-B)] colors are -0.49, 0.06, -0.03 (-0.39, 0.01, 0.69). Thus by including GALEX measurements we gain a finer resolution for parameters of young associations and complexes, hence a clearer, unbiased census of recent star formation. Figure 4 indicates that SF in M101 occured over the last 10^9 yrs, both in stellar clusters (Chandar et al. 2004) and in larger complexes (GALEX results, this paper). This analysis will be extended to other resolved galaxies in the GALEX NGS, to compare their cluster systems and star-formation histories.

4. The properties of the stellar populations

To explore the average properties of the stellar population as a function of galactocentric distance, we computed radial profiles of the FUV and NUV median surface brightness for each galaxy within concentric elliptical annuli, oriented in accordance with the galaxy inclination and position angle (M101: i=18^o, PA=39^o, Bosma et al. 1981; M51: i=20^o, PA=170^o, Rots et al. 1990). Within each annulus we measured the median surface brightness (thus removing the discrete peaked sources, and the foreground stars) and subtracted an average sky background, determined in a wide elliptical annulus exterior to the galaxy. In Figure 5 we plot the surface brightness as a function of radius in the two GALEX bands, as well as the FUV-NUV color. Values of this color for SSP and CSP models are indicated for a range of ages. As shown previously, this color is essentially reddening-free, thus gives a direct indication of the age. Observed colors are redder than CSP models for a wide range

of ages, across most of the galaxy, excluding this scenario. SSP models represent the extreme opposite of the CSP scenario, and SSP ages have only indicative value, since we are comparing colors of azimuthally averaged populations, and single bursts of star formation (clusters, associations) would likely be localized. The SSP ages indicate a more recent star-formation activity towards outer regions (spanning two dex in age) for M101, and much less conspicuous fluctuations in M51, while the bulge has an older (average) age. The comparison of Figure 5 with the FUV radial profile from UIT data (Kuchinski et al. 2000) shows the advantage of the GALEX measurements. In addition to providing the FUV -NUV color, for both M101 and M51 the profiles in Figure 5 extend to larger galactocentric radii, sampling outer disk areas, about 3 magnitudes fainter than the UIT data (note again that we use AB magnitudes, which differ from the UIT magnitude system - for FUV - by ≈ 2.8 mag).

The radial profiles of the FUV -NUV color in the Local Group galaxies M 33 and M 31, and in M83, (Thilker et al, 2004a,b this issue) show the same trend of the FUV -NUV color becoming bluer outwards, the magnitude of the color gradient differing from galaxy to galaxy. An extensive comparison among a representative sample of nearby galaxies will follow in a forthcoming paper.

Acknowledgement:

GALEX (Galaxy Evolution Explorer) is a NASA Small Explorer, launched in April 2003. We gratefully acknowledge NASA's support for construction, operation, and science analysis of the GALEX mission, developed in cooperation with the Centre National d'Etudes Spatiales of France and the Korean Ministry of Science and Technology. We are very grateful to R. Chandar for helpful discussions, and to the referee for many useful suggestions.

REFERENCES

Bertin, E. and Arnouts, S., 1996, A&AS, 117, 393

Bianchi, L., Madore, B., Thilker, D., Gil de Paz, A., and Martin, C., 2004a, in "The Local Group as an Astrophysical Laboratory", in press

Bianchi, L., Madore, B., Thilker, D., Gil de Paz, A., and the GALEX team, 2004b, AAS 203, 91.12

Bianchi, L., Chandar, R., Ford, H. 1999: Mem. SAIT, eds. D.de Martino & L. Buson, Vol. 70 N.2, p. 629

Bosma, A. , Goss, W. M., Allen, R. J., 1981, A&A93, 106

Bruzual, G. & Charlot, G., 2003, MNRAS, 344, 1000

Chabrier, G., 2003, PASP, 115, 763

Chandar, R., Bianchi, L., Ford, H. and Salasnich, B. 1999, PASP, 111, 794

Chandar, R., et al. 2004, in preparation

Freedman, W. L., Wilson, C. D., & Madore, B. F. 1991, ApJ, 372, 455

Hill, J.K., et al. 1997, ApJ, 477, 673

Hoopes, C., Walterbros, R., Bothun, G. 2001, ApJ, 559, 2001

Kelson, D. D., et al. 1996, ApJ, 463, 26

Kennicutt, R., Bresolin, F., & Garnett, 2003, ApJ591, 801

Kuchinski, L.E., et al. 2000, ApJS, 131, 441

Martin, D. C., et al. 2004, ApJ, present volume

Morrissey, P., et al. 2004, ApJ, present volume

Rots, A. H., Crane, P. C., Bosma, A., Athanassoula, E., van der Hulst, J. M., 1990, AJ, 100, 337

Sandage, A., & Tammann, G. A. 1974, ApJ, 194, 559

Thilker, D., Bianchi, L., et al. 2004a, ApJ, present volume

Thilker, D., Hoopes, C., Bianchi, L., et al. 2004b, ApJ, present volume

Waller, W.H., et al. 1997, ApJ, 481, 169

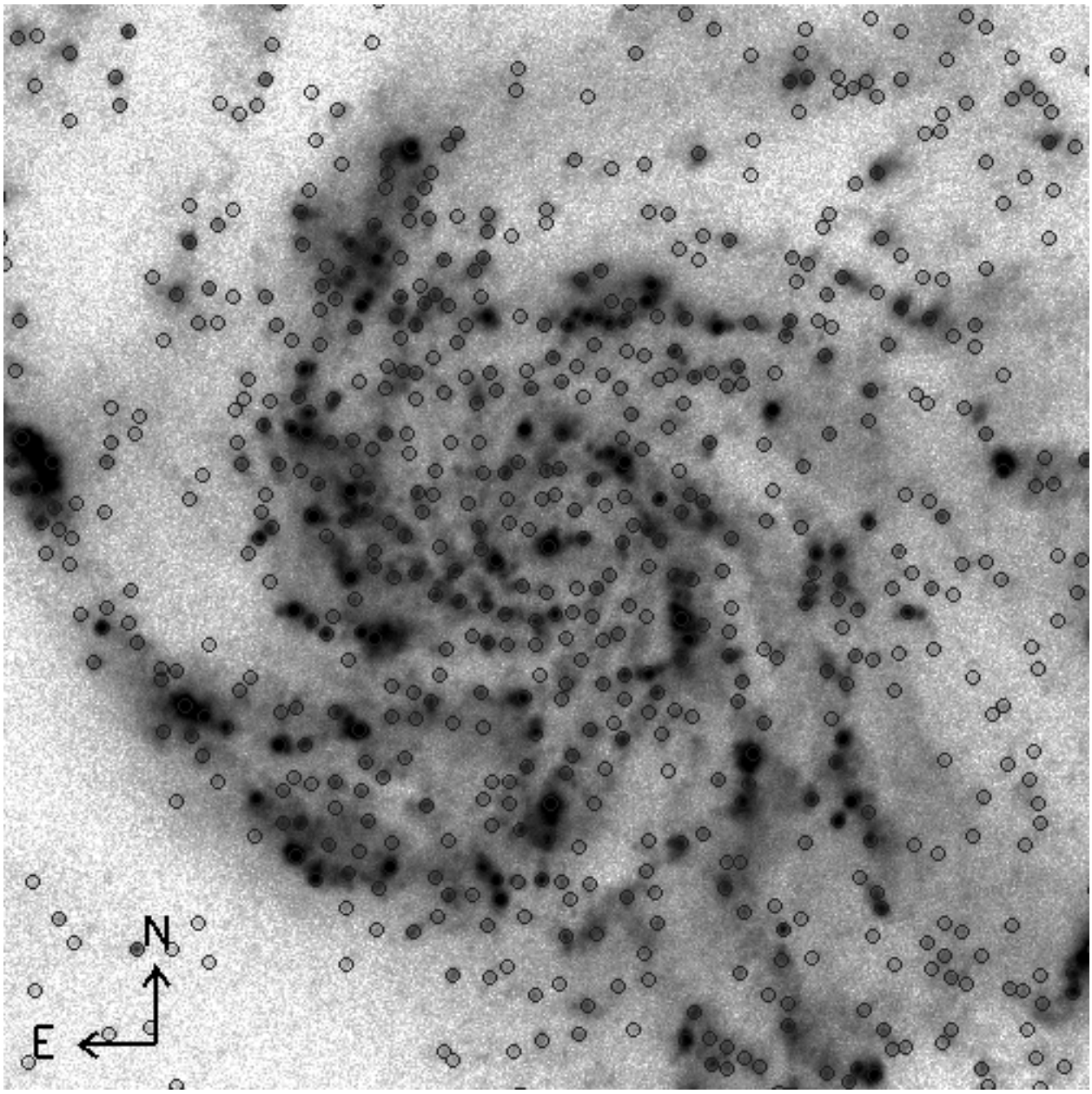

Fig. 1.— A portion (12.5′ square) of a GALEX-NUV image of M101. The compact UV sources with photometric errors <0.2 mag are indicated with circles.

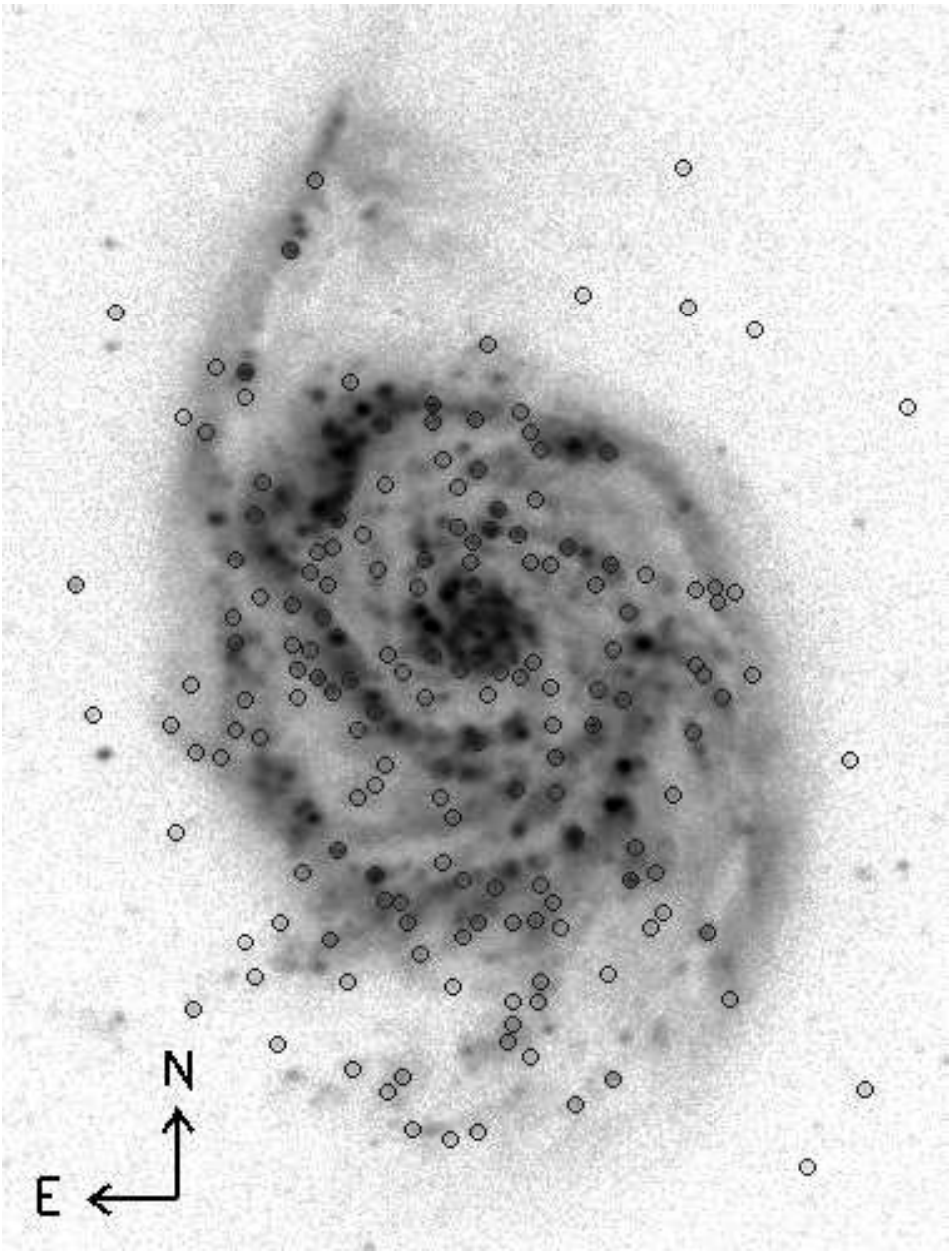

Fig. 2.— Same as Fig. 1, for M51 (9.5x12.5′).

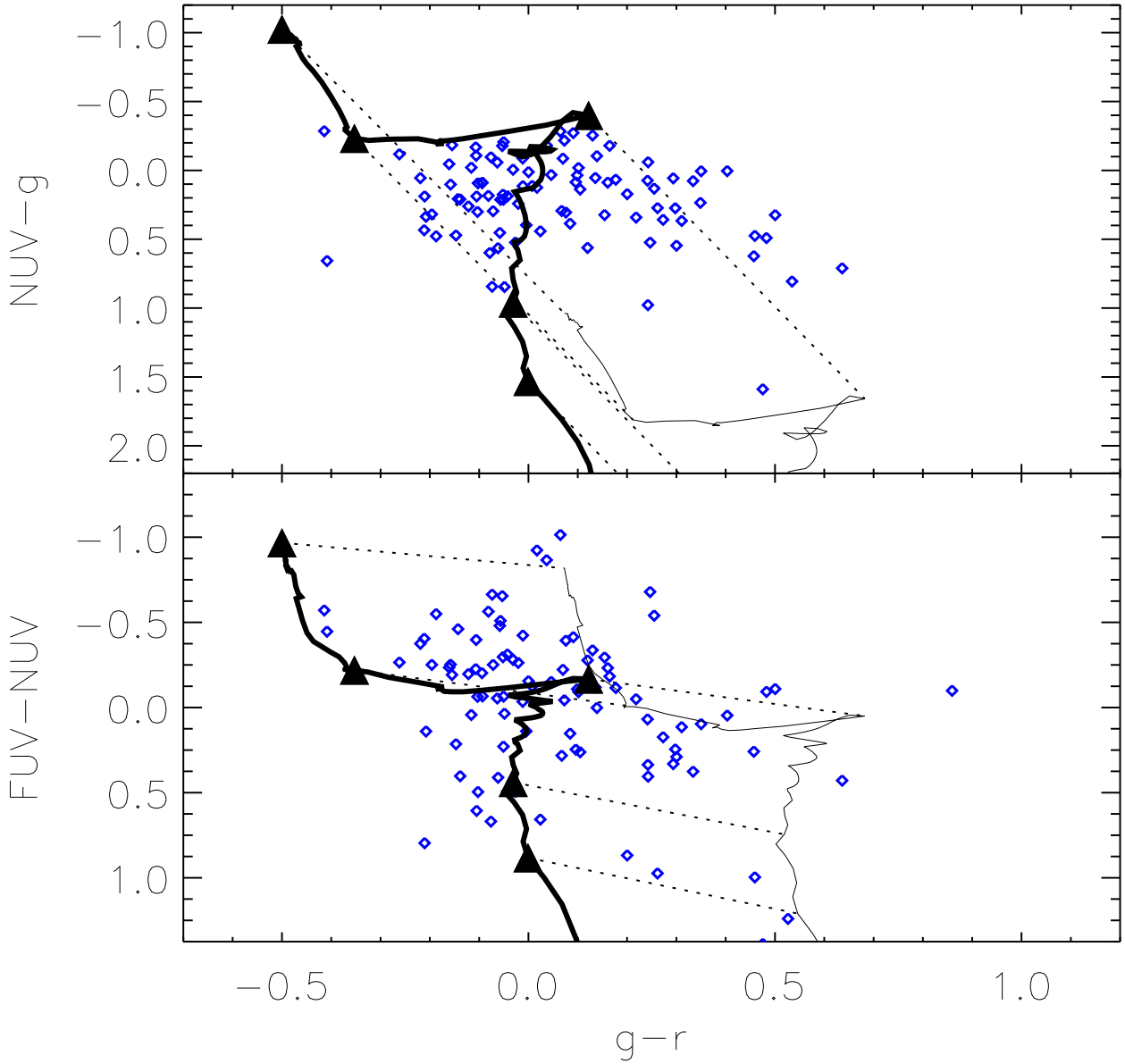

Fig. 3.— Color-color diagrams for the compact UV sources in M101. Only sources with photometric errors <0.1 mag (GALEX bands) and <0.05 mag (SDSS bands) are plotted. The solid black curve shows the intrinsic colors for SSP models as a function of age. Model colors reddened with E(B-V)=0.5 are shown with a thin black line (dotted lines connect the intrinsic and reddened color for the same model at representative ages). Filled black triangles mark ages (in log years) of 6.0, 6.7, 6.9, 8.0, 8.3.

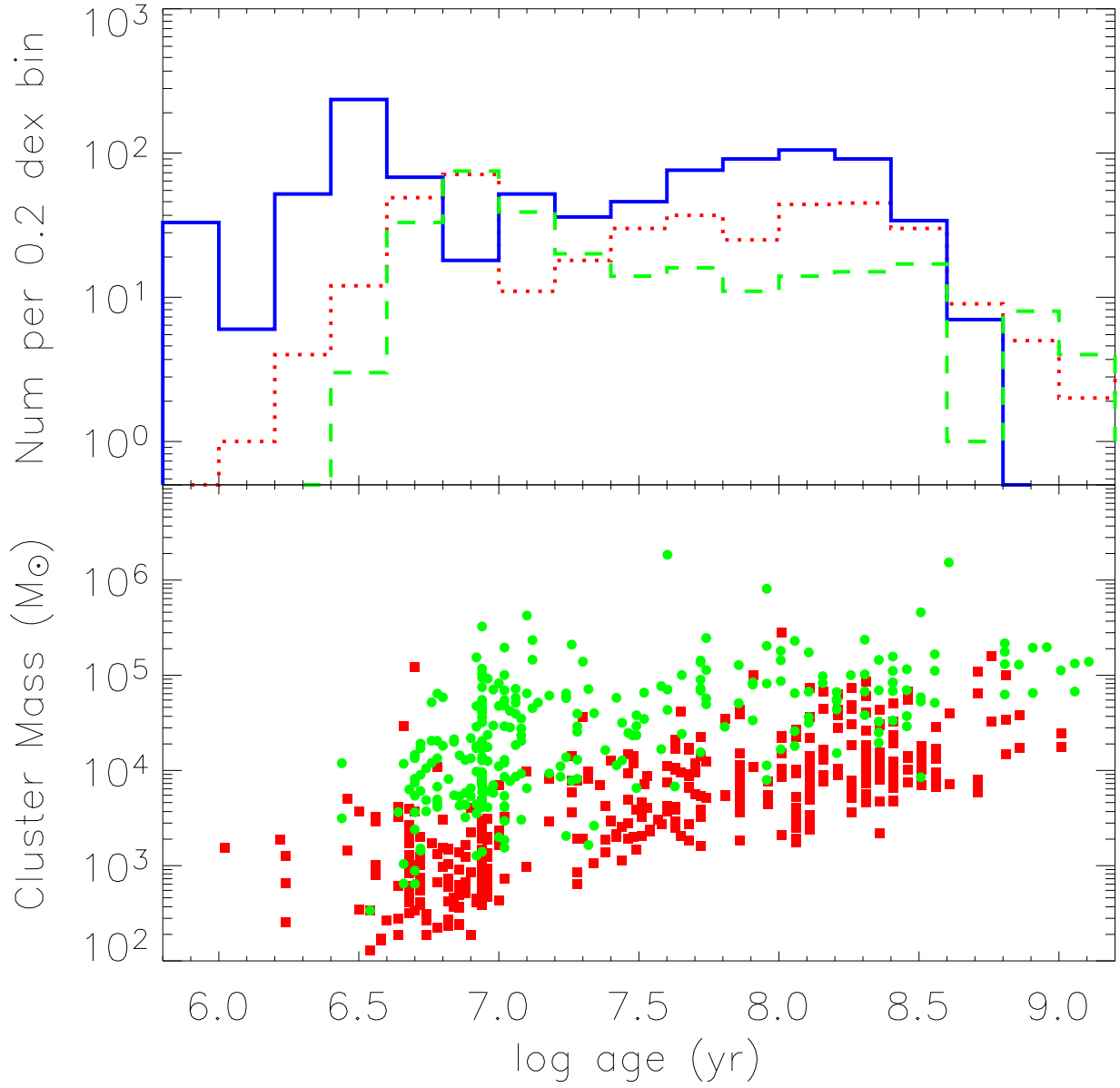

Fig. 4.— Top: histogram of the derived ages for the compact stellar complexes in M101 from SED fits (dashed green) and from *FUV* -*NUV* color only (solid blue). Only sources with small photometric errors and good SED fits are included in the green sample, limiting the sample to about 300 sources. All sources with errors <0.2 mag in *FUV* and *NUV* bands are included in the blue (solid) histogram (about 1100 sources). The truncation at ages $<10^9$ yrs for the blue histogram (*FUV* -*NUV*) is a selection effect of the sample. The

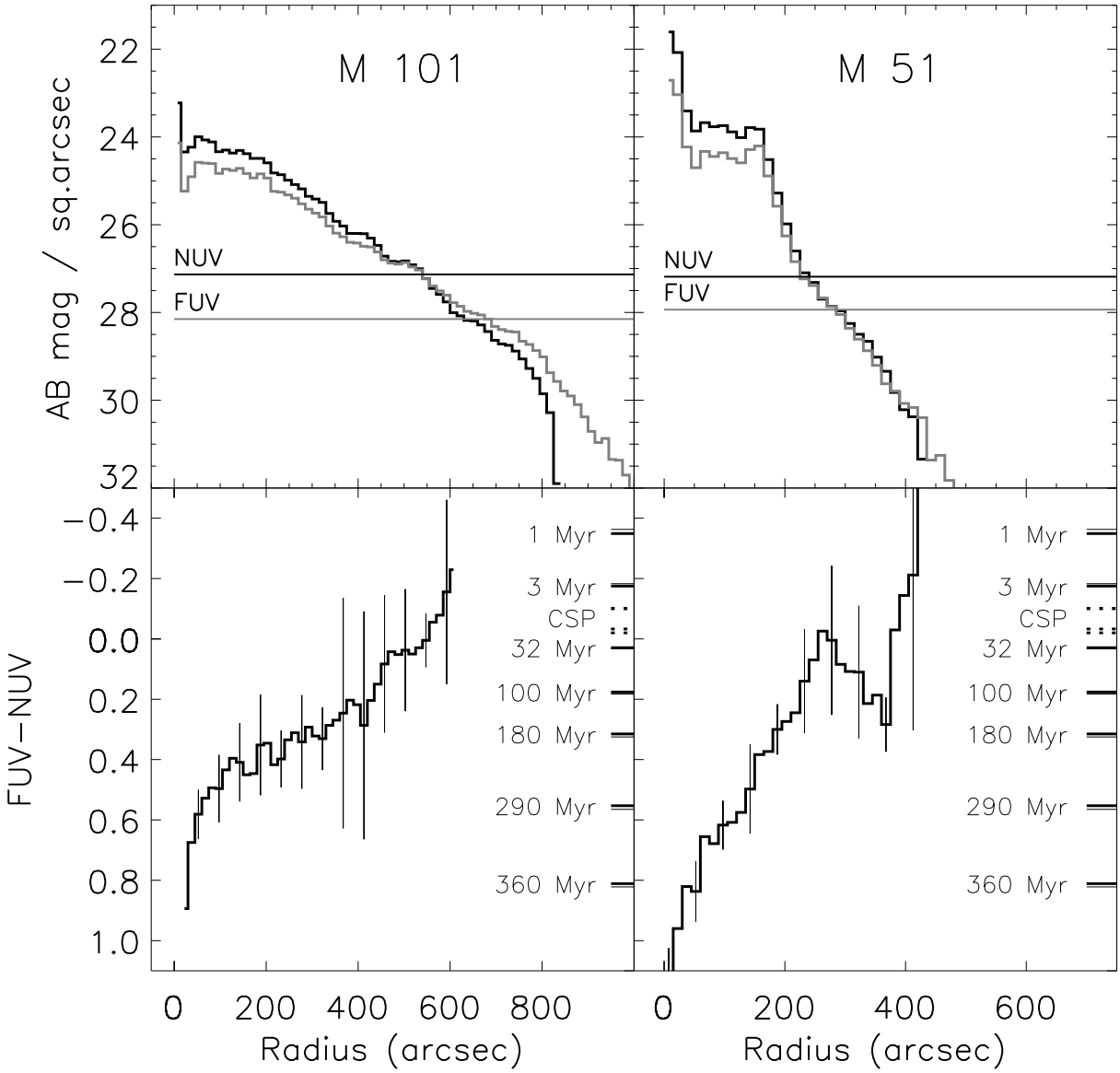

Fig. 5.— Radial profiles of *FUV* and *NUV* median surface brightness, and FUV-NUV color. Errors ($\pm$ 1 σ) are shown for representative points of the FUV-NUV color. For the brightness profiles, errors range between 0.075 to 0.3 mag in the range 24-29 mag. The horizontal lines are the estimated sky surface brightness in each band. On the *FUV* -*NUV* panels, we show (line segments) theoretical *FUV* -*NUV* values for SSP models of ages 1, 3, 32, 100, 180, 290, 360 Myr, and CSP models of ages 0.1, 1, 10 Gyr (dashed segments).

Table 1. The sample of sources in the different bands

Band	Sources (error<0.2 mag)	Mag.lim.	Sources (error<0.1 mag)	Mag.lim.	Sources (error<0.05 mag)	Mag.lim.
M 101						
FUV	1034	22.1	383	20.8	82	19.1
NUV	2179	22.8	898	21.7	249	20.4
u	1351	22.4	878	21.7	389	20.6
g	1315	23.0	939	22.3	539	21.4
r	1233	22.6	851	22.0	467	21.2
i	1066	22.4	715	21.6	419	20.4
z	796	21.1	468	20.4	248	19.1
M 51						
FUV	200	22.5	78	21.1	25	19.6
NUV	622	22.9	257	21.9	83	20.7
u	268	—	140	21.8	54	20.7
g	253	—	153	22.5	76	21.6
r	228	—	131	21.9	71	21.0
i	205	—	115	21.7	65	20.6
z	170	—	85	20.2	42	19.3